

# Journal of Biomedical Optics

[SPIEDigitalLibrary.org/jbo](http://SPIEDigitalLibrary.org/jbo)

## ***In vivo* near-infrared dual-axis confocal microendoscopy in the human lower gastrointestinal tract**

Wibool Piyawattanametha  
Hyejun Ra  
Zhen Qiu  
Shai Friedland  
Jonathan T. C. Liu  
Kevin Loewke  
Gordon S. Kino  
Olav Solgaard  
Thomas D. Wang  
Michael J. Mandella  
Christopher H. Contag

# *In vivo* near-infrared dual-axis confocal microendoscopy in the human lower gastrointestinal tract

Wibool Piyawattanametha,<sup>a,b,c,\*</sup> Hyejun Ra,<sup>a,\*</sup> Zhen Qiu,<sup>d</sup> Shai Friedland,<sup>e</sup> Jonathan T. C. Liu,<sup>f</sup> Kevin Loewke,<sup>a</sup> Gordon S. Kino,<sup>g</sup> Olav Solgaard,<sup>g</sup> Thomas D. Wang,<sup>d</sup> Michael J. Mandella,<sup>a</sup> and Christopher H. Contag<sup>a</sup>

<sup>a</sup>Stanford University, James H. Clark Center for Biomedical Engineering & Sciences, Departments of Pediatrics, Radiology and Microbiology & Immunology, Molecular Imaging Program, Stanford, California 94305

<sup>b</sup>National Electronics and Computer Technology Center, Pathumthani, Thailand 12120

<sup>c</sup>Chulalongkorn University, Advanced Imaging Research Center, Faculty of Medicine, Pathumwan, Thailand 10330

<sup>d</sup>University of Michigan, Department of Biomedical Engineering, Ann Arbor, Michigan 48109

<sup>e</sup>Stanford University, Palo Alto Veterans Hospital, Stanford, California 94305

<sup>f</sup>Stony Brook University (SUNY), Department of Biomedical Engineering, Stony Brook, NY 11794

<sup>g</sup>Stanford University, Edward L. Ginzton Laboratory, Stanford, California 94305

**Abstract.** Near-infrared confocal microendoscopy is a promising technique for deep *in vivo* imaging of tissues and can generate high-resolution cross-sectional images at the micron-scale. We demonstrate the use of a dual-axis confocal (DAC) near-infrared fluorescence microendoscope with a 5.5-mm outer diameter for obtaining clinical images of human colorectal mucosa. High-speed two-dimensional *en face* scanning was achieved through a micro-electromechanical systems (MEMS) scanner while a micromotor was used for adjusting the axial focus. *In vivo* images of human patients are collected at 5 frames/sec with a field of view of  $362 \times 212 \mu\text{m}^2$  and a maximum imaging depth of  $140 \mu\text{m}$ . During routine endoscopy, indocyanine green (ICG) was topically applied a nonspecific optical contrasting agent to regions of the human colon. The DAC microendoscope was then used to obtain micro-anatomic images of the mucosa by detecting near-infrared fluorescence from ICG. These results suggest that DAC microendoscopy may have utility for visualizing the anatomical and, perhaps, functional changes associated with colorectal pathology for the early detection of colorectal cancer. © 2012 Society of Photo-Optical Instrumentation Engineers (SPIE). [DOI: 10.1117/1.JBO.17.2.021102]

Keywords: confocal; dual-axis; Gastrointestinal Tract; MEMS; microendoscope; near-infrared fluorescence.

Paper 113355S received Jul. 4, 2011; revised manuscript received Sep. 9, 2011; accepted for publication Sep. 9, 2011; published online Mar. 2, 2012.

## 1 Introduction

Colorectal cancer is one of the most common cancers, ranking third worldwide in frequency of incidence after cancers of the lung and breast.<sup>1</sup> There are over 1.2 million new cases each year and over 600,000 individuals will eventually die from this malignancy. Survival rates depend largely on the stage of diagnosis. Statistics show that about 90% of patients diagnosed with localized cancer survive beyond 5 years, compared with 68% of those diagnosed with regional disease.<sup>2</sup> Therefore, there is a pressing need to detect colorectal cancer at early stages, with the aim to improve prognosis and reduce mortality.

Confocal microscopy is an optical imaging technique that has been widely used in various biological and biomedical applications.<sup>3</sup> This imaging modality can generate high-resolution (micron-scale) cross-sectional images of biological tissues. The high axial resolution provided by confocal microscopy allows imaging of thin “optical sections” within live intact tissue. Typically, either reflectance or fluorescence images can be collected to identify morphological or molecular features, respectively, of cells and tissues.

The development of confocal microendoscopy has been accelerated by advances and cost reductions in its photonic components, such as optical fibers and diode lasers, as well

as microfabrication technologies, including laser beam-scanning micromirrors. These microendoscopes are being integrated in to a wide range of medical devices, including catheters, endoscopes, and surgical instruments, with the goal of enabling *in vivo* imaging inside the human body for early disease detection, the staging of lesions, and guiding therapies.<sup>4–6</sup>

## 2 Dual-Axis Confocal Microendoscope Architecture

The aforementioned efforts present great technical challenges for satisfy the demanding specifications for high axial resolution, deep penetration depth, high contrast, and fast frame rates in miniature devices. A variety of miniature configurations,<sup>7,8</sup> including single<sup>9</sup> and multiple fiber<sup>4</sup> strategies, have been devised to meet some of these requirements. Thus far, miniature confocal microscopes have all employed a conventional single-axis architecture with the illumination and collection paths aligned along the same optical axis. Excellent lateral resolution can be achieved using a sufficiently high numerical aperture (NA) lens at the expense of a limited working distance (WD) and field-of-view (FOV), which decreases as the lens is scaled down in size. Therefore, due to the limited WD of a high-NA lens, the beam-scanning mechanisms of confocal scanning microscopes are typically located proximal to the objective lens (i.e., preobjective position). Unfortunately, preobjective beam scanning leads to off-axis aberrations, such as coma and

\*Authors contributed equally to this work.

Address all correspondence to: Wibool Piyawattanametha, Chulalongkorn University, Advanced Imaging Research Center, Faculty of Medicine, Pathumwan, Thailand 10330. Tel: 662-363-7634; E-mail: wibool@gmail.com

astigmatism, that require mitigation through complex optical designs.

The dual-axis confocal (DAC) configuration was developed to overcome these limitations for endoscope compatibility and *in vivo* imaging by utilizing two optical fibers oriented along intersecting optical axes of two low-NA objectives in order to spatially separate the light paths for illumination and collection.<sup>10,11</sup> The overlapping region between the foci of the two beams defines the focal volume, and, hence, the resolution, which is sub-cellular in all three dimensions. Furthermore, low-NA objectives enable an increased WD, such that a scanning mirror can be located on the distal side of the lens (i.e., postobjective position), thus eliminating off-axis aberrations. In other words, the beams always pass through the low-NA objectives in a direction that is collinear to the optical axis of each lens, resulting in a diffraction-limited focus that can then be scanned over a large FOV by a nonaberrating mirror surface. This configuration allows the instrument to be scaled down in size to millimeter dimensions for compatibility with medical endoscopes. Furthermore, the DAC configuration has been shown through Monte-Carlo simulations, tissue-phantom experiments, and imaging studies to enable superior rejection of out-of-focus and multiply scattered light in thick tissues.<sup>12</sup>

### 3 DAC Microendoscope Components and Performance

The design and integration of our microscope requires a package that allows for precise alignment of the following optical elements: (1) two fiber-coupled collimators, (2) a two-dimensional (2D) microelectromechanical (MEMS) scanner,<sup>13</sup> (3) a parabolic focusing mirror, and (4) a hemispherical index-matching solid immersion lens (SIL). The basic design of the microendoscope scanhead is shown in Fig. 1(a). The 5-mm-diameter parabolic mirror (NA = 0.5) is fabricated using a replicated molding process that provides the high-quality surface profile that is needed for diffraction-limited focusing of two collimated beams. Once the beams are aligned parallel to each other, the parabolic mirror then causes the focused beams to intersect at a common focal point below the tissue surface. Since each of the two collimators are only 1 mm in diameter, the collimated beams underfill the parabolic mirror where they are focused with an effective NA of 0.1.

The components used in earlier handheld microscopes<sup>14–16</sup> were used in the 5.5-mm diameter microendoscope package, which is based on the design shown in Fig. 1. This smaller prototype uses the same replicated parabolic focusing mirror but with a smaller diameter (5 mm). The MEMS scanner being used in this microendoscope is also similar in design to the one employed in previous 10-mm diameter handheld versions of the DAC microscope. A pair of 1-mm diameter fiber-coupled gradient-index (GRIN) collimating lenses, which were reduced in diameter from 1.8 mm, are employed in this DAC microendoscope. In order for the illumination and collection beams to intersect and focus at a single point in space, the collimated beams must be made exactly parallel to each other prior to impinging upon the parabolic focusing mirror. Beam alignment is achieved by manually rotating a pair of 1-mm diameter Risley prisms that are inserted into the path of one of the collimated beams. The collimators and Risley prisms are both held by precision wire-electrical discharge machined (EDM) v-grooves and fixed in place with a UV-curing epoxy. As with the larger prototypes, the combined precision of the v-grooves and the pointing accuracy of the preassembled fiber collimators allow for the collimated beams to be made parallel to each other to within 0.05 deg. The Risley prisms have a small wedge angle (0.1 deg), allowing the collimated beams to be steered over a range of 0.05 deg such that the beams are perfectly parallel with each other. Fig. 2(a) shows a fully packaged DAC microendoscope that is distally loaded through the instrument channel of an Olympus XT-160 therapeutic upper endoscope (6-mm diameter instrument channel). Fig. 2(b) shows the distal end of an endoscope with the DAC microendoscope protruding out of the instrument channel.

The MEMS mirror is electrostatically actuated to raster scan. Both the illumination and collection beams with one of its axis oscillate at resonance (1.1 kHz with an actuation voltage of 90 V) and the orthogonal axis oscillates near DC (1 to 5 Hz with actuation voltage of 170 V). The differential drive is performed on the MEMS driving bias in order to maximize linearization of the beam trajectory.<sup>17</sup> Each 2D *en face* image is continuously displayed on a computer monitor with a custom frame grabber, using National Instruments (NI) data acquisitions boards (NI models: PXI-6711 and PXI-6251) that are controlled using LabVIEW. A computer-controlled micromotor within the microscope package is used to actuate an axial sliding mechanism

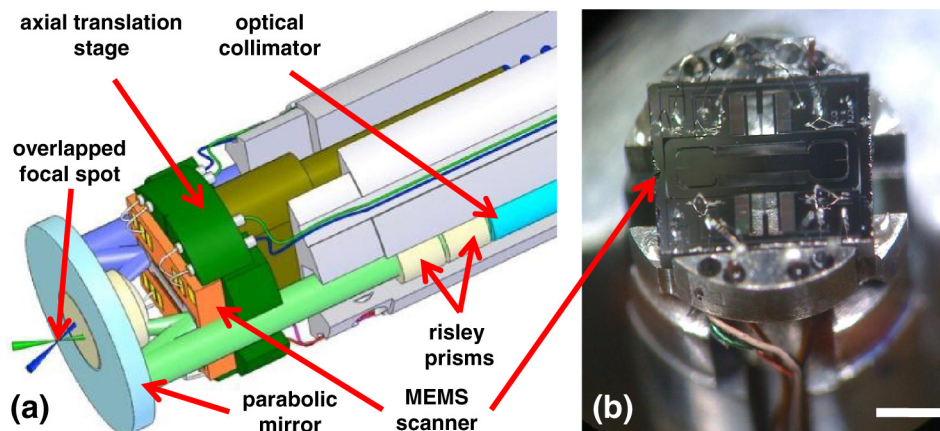


**Fig. 1** A 5.5-mm diameter DAC microendoscope scanhead. (a) Two collimated beams are focused by a parabolic mirror. Real-time *en face* scanning is performed by a 2-D MEMS scanner. (b) Photograph of the microendoscope without its cap showing a 2-D MEMS scanner mounted on the axial translation stage; Scale bar = 3 mm.

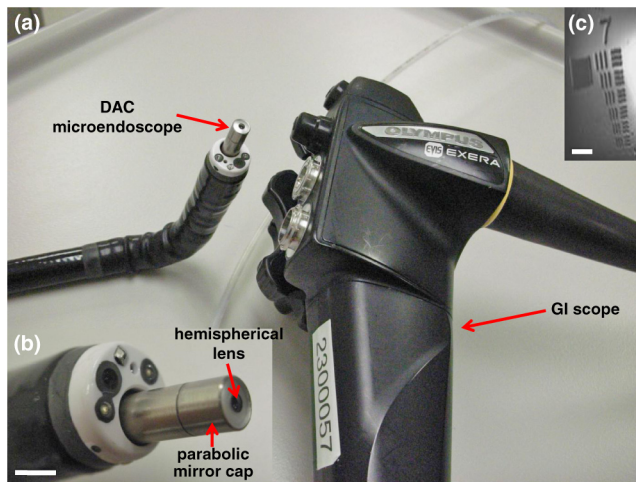


**Fig. 2** (a) A DAC microendoscope is passed through the instrument channel of an Olympus XT-160 endoscope that has a 6-mm diameter instrument channel. (b) Distal end of an endoscope showing the protruding DAC microendoscope; Scale bar = 5 mm. (c) Cropped reflectance image of a 1951 United States Air Force resolution test chart collected using the DAC microendoscope. Shows a transverse resolution of  $5\ \mu\text{m}$ ; Scale bar =  $20\ \mu\text{m}$ .

that serves as the MEMS mirror mount, thus providing real-time imaging-depth adjustments. The micromotor (Faulhaber GmbH & Co. KG) consists of a brushless DC motor (model 0308), a micro-planetary gearhead (model 03A), and a linear actuator (model 03A-S3). Each 3D volumetric image is created using postprocessing to render a series of 2D *en face* images. A near-infrared laser light source with a center wavelength of 785 nm was used in this experiment. Imaging was performed in either the reflectance or fluorescence mode; in the latter case, a 790-nm long-pass optical filter is inserted in to the collection path. The maximum laser power directed at the sample is 3.6 mW with a FOV of  $362 \times 212\ \mu\text{m}^2$  ( $500 \times 295$  pixels). The axial resolution is  $6.5\ \mu\text{m}$ , as measured by axially translating a reflecting surface through the focal plane. The transverse resolution is  $5\ \mu\text{m}$ , as derived from the reflectance images shown in Fig. 2(c).

## 4 Experimental Results and Conclusion

### 4.1 *Ex vivo* Fluorescence Images

The 3D fluorescence imaging capability of the handheld dual-axis confocal instrument is shown in Fig. 3. Excised tissue specimens from normal and dysplastic colonic mucosa were soaked in 0.5 mg IRDye® 800 continuous-wave *N*-hydroxysuccinimide (CW NHS) Ester (LI-COR Biosciences, Inc) diluted in 10 ml of phosphate-buffered saline (PBS) at neutral pH for 5 min and then rinsed with PBS to remove excess dye. After imaging, the specimens were fixed in 10% buffered formalin, embedded in paraffin, cut into  $5\text{-}\mu\text{m}$  sections, and processed for histology with hematoxylin and eosin (H&E) staining. All *ex vivo* images were obtained from freshly excised human tissues (after informed consent and institutional review board approval was obtained from Stanford University and the Veterans Affairs Palo Alto Health Care System). Fig. 3(a)–(c) show the *en face* image, H&E, and 3D volumetric images of normal colonic mucosa, respectively. The features of the colonic crypts, including colonocytes and crypt lumens, are clearly

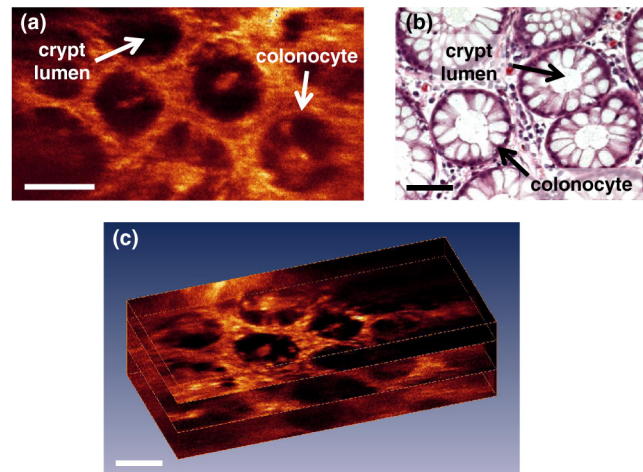


**Fig. 3** *Ex vivo* fluorescence images obtained using a DAC microendoscope. *En face* image of (a) normal colonic mucosa, (b) corresponding histology (H&E) of (a), and (c) 3D volumetric image of (a). Scale bar =  $100\ \mu\text{m}$ .

resolved. Fig. 3(c) shows three extracted *en face* planes at 30, 90, and  $140\ \mu\text{m}$  below the tissue surface. The photomultiplier tube (PMT) gain was increased with depth in order to compensate for signal attenuation.

### 4.2 *In vivo* Fluorescence Images

Real-time *in vivo* fluorescence imaging was performed in the colons of human patients with our DAC microendoscope. While performing standard video colonoscopy, the confocal images were simultaneously collected from the MEMS-based microendoscope, which occupied the instrument channel of the endoscope. Before each imaging session, lyophilized indocyanine green (ICG) (Akorn, Inc.) was dissolved in an aqueous solvent (5 mg/ml) and was topically applied to the gastrointestinal (GI) mucosal surface for 2–3 min before washing out the

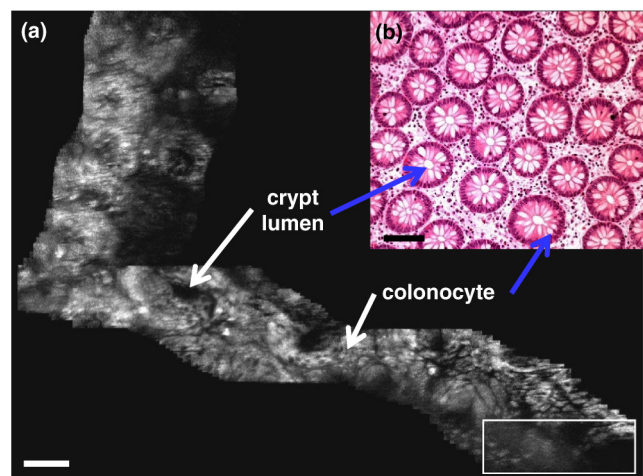


**Fig. 4** A mosaic of approximately 180 individual *en face* images. (a) Image collected with the DAC microendoscope (post processed) of normal colonic mucosa at a depth of  $60\ \mu\text{m}$  (Video 1) and (b) a representative histologic (H&E) image of normal colonic mucosa. Scale bar =  $100\ \mu\text{m}$ . The white rectangle represents an individual *en face* image ( $362\ \mu\text{m} \times 134\ \mu\text{m}$ ) obtained using the DAC microendoscope (Video 1, 4.2 MB MPEG). [URL: <http://dx.doi.org/10.1117/1.JBO.17.2.021102.1>]

excess dye with water. Fig. 4(a) shows a sequence of approximately 180 individual *en face* mosaiced images (post processed) of normal colonic mucosa acquired at a depth of 60  $\mu\text{m}$  beneath the mucosal surface. The white rectangle represents an individual *en face* image ( $362 \times 134 \mu\text{m}^2$ ;  $500 \times 190$  pixels) obtained with the DAC microendoscope. Normal colonic microarchitecture is seen as circular and regularly spaced crypts that line the epithelial layer [Fig. 4(a)]. The images were mosaiced by first correcting the image borders for scanning distortions. Then, each new image was registered and merged before proceeding to the subsequent image.<sup>18</sup> Fig. 4(b) shows a representative histologic image derived from H&E staining of normal colonic mucosa. After each use, the whole microendoscope is soaked in Cidex Solution (Civco Medical Solutions, Inc.) for 45 min at room temperature in order to disinfect and sterilize the imaging probe.

In summary, we have engineered the first MEMS-based DAC microendoscope (5.5-mm diameter) to be used for obtaining near-infrared fluorescence images *in vivo* from the colon of human patients. This MEMS-based microendoscope is a step towards enabling point-of-care pathology for the *in vivo* diagnosis, staging of colorectal lesions, and guiding biopsies and therapies.

### Acknowledgments

WP was partially supported by grants from the National Research Council, the Higher Education Research Promotion & National Research University Project, and the Office of the Higher Education Commission of Thailand (HR1162A and HR1166I). This work was supported in part by grants from the National Institutes of Health, including U54 CA105296, R33 CA109988, K08 DK67618, P50 CA93990, and U54 CA136429.

### References

1. A. Jemal, F. Bray, M. M. Center, J. Ferlay, E. Ward, and D. Forman, "Global cancer statistics," *CA. Cancer J. Clin.* **61**(2), 69–90 (2011).
2. N. Howlader, A. M. Noone, M. Krapcho, N. Neyman, R. Aminou, W. Waldron, S. F. Altekruse, C. L. Kosary, J. Ruhl, Z. Tatalovich, H. Cho, A. Mariotto, M. P. Eisner, D. R. Lewis, H. S. Chen, E. J. Feuer, K. A. Cronin, and B. K. Edwards, *Seer cancer statistics review, 1975-2008*, National Cancer Institute, Bethesda, MD (2011).
3. T. R. Corle and G. S. Kino, *Confocal scanning optical microscopy and related imaging systems*, Academic Press, San Diego (1996).
4. E. Laemmel, M. Genet, G. Le Goualher, A. Perchant, J. F. Le Gargasson, and E. Vicaut, "Fibered confocal fluorescence microscopy (cell-vizio) facilitates extended imaging in the field of microcirculation. A comparison with intravital microscopy," *J. Vasc. Res.* **41**(5), 400–411 (2004).
5. N. Thekkekk and R. Richards-Kortum, "Optical imaging for cervical cancer detection: solutions for a continuing global problem," *Nat. Rev. Cancer* **8**(9), 725–731 (2008).
6. D. P. Hurlstone, N. Tiffin, S. R. Brown, W. Baraza, M. Thomson, and S. S. Cross, "In vivo confocal laser scanning chromo-endomicroscopy of colorectal neoplasia: Changing the technological paradigm," *Histopathology* **52**(4), 417–426 (2008).
7. D. L. Dickensheets and G. S. Kino, "Silicon-micromachined scanning confocal optical microscope," *IEEE J. Microelectromech. Syst.* **7**(1), 38–47 (1998).
8. A. D. Aguirre, P. R. Hertz, Y. Chen, J. G. Fujimoto, W. Piyawattanametha, L. Fan, and M. C. Wu, "Two-axis mems scanning catheter for ultrahigh resolution three-dimensional and *en face* imaging," *Opt. Express* **15**(5), 2445–2453 (2007).
9. P. M. Delaney, M. R. Harris, and R. G. King, "Fiber-optic laser scanning confocal microscope suitable for fluorescence imaging," *Appl. Opt.* **33**(4), 573–577 (1994).
10. T. D. Wang, M. J. Mandella, C. H. Contag, and G. S. Kino, "Dual-axis confocal microscope for high-resolution *in vivo* imaging," *Opt. Lett.* **28**(6), 414–416 (2003).
11. W. Piyawattanametha and T. D. Wang, *In vivo microendoscopy*, McGraw Hill Professional, New York, NY, 45–76 (2011).
12. J. T. C. Liu, M. J. Mandella, J. M. Crawford, C. H. Contag, T. D. Wang, and G. S. Kino, "Efficient rejection of scattered light enables deep optical sectioning in turbid media with low-numerical-aperture optics in a dual-axis confocal architecture," *J Biomed Opt* **13**(3), 034020 (2008).
13. H. Ra, W. Piyawattanametha, Y. Taguchi, D. Lee, M. J. Mandella, and O. Solgaard, "Two-dimensional mems scanner for dual-axes confocal microscopy," *IEEE J. Microelectromech. Syst.* **16**(4), 969–976 (2007).
14. J. T. C. Liu, M. J. Mandella, H. Ra, L. K. Wong, O. Solgaard, G. S. Kino, W. Piyawattanametha, C. H. Contag, and T. D. Wang, "Miniature near-infrared dual-axes confocal microscope utilizing a two-dimensional microelectromechanical systems scanner," *Opt. Lett.* **32**(3), 256–258 (2007).
15. H. Ra, W. Piyawattanametha, M. J. Mandella, P.-L. Hsiung, J. Hardy, T. D. Wang, C. H. Contag, G. S. Kino, and O. Solgaard, "Three-dimensional *in vivo* imaging by a handheld dual-axes confocal microscope," *Opt. Express* **16**(10), 7224–7232 (2008).
16. W. Piyawattanametha, H. Ra, M. J. Mandella, K. Loewke, T. D. Wang, G. S. Kino, O. Solgaard, and C. H. Contag, "3-d near-infrared fluorescence imaging using an mems-based miniature dual-axis confocal microscope," *IEEE J. Sel. Top. Quantum Electron.* **15**(5), 1344–1350 (2009).
17. W. Piyawattanametha, R. P. J. Barretto, T. H. Ko, B. A. Flusberg, E. D. Cocker, H. J. Ra, D. S. Lee, O. Solgaard, and M. J. Schnitzer, "Fast-scanning two-photon fluorescence imaging based on a microelectromechanical systems two-dimensional scanning mirror," *Opt. Lett.* **31**(13), 2018–2020 (2006).
18. K. E. Loewke, D. B. Camarillo, W. Piyawattanametha, M. J. Mandella, C. H. Contag, S. Thrun, and J. K. Salisbury, "In vivo micro-image mosaicing," *IEEE Trans. Biomed. Eng.* **58**(1), 159–171 (2011).